Forward Physics Facility

M. V. Diwan

Physics Department

Brookhaven National Laboratory

U.S. Department of Energy
USDOE Office of Science (SC), High Energy Physics (HEP) (SC-25)

DISCLAIMER

FORWARD PHYSICS FACILITY

FPF Working Groups

Working Group Conveners: Luis A. Anchordoqui,[1] Akitaka Ariga,[2,3] Tomoko Ariga,[4] Alan J. Barr,[5] Brian Batell,[6] Jianming Bian,[7] Jamie Boyd,[8] Matthew Citron,[9] Giovanni De Lellis,[10,11] Albert De Roeck,[8] Antonia Di Crescenzo,[8,10,11] Milind V. Diwan,[12] Jonathan L. Feng,[7] Christopher S. Hill,[13] Felix Kling,[14] Steven Linden,[15] Josh McFayden,[16] Hidetoshi Otono,[4] Mary Hall Reno,[17] Juan Rojo,[18,19] Dennis Soldin,[20] Sebastian Trojanowski,[21,22] and Wenjie Wu[7]

[1]*Department of Physics and Astronomy, Lehman College, City University of New York, Bronx, NY 10468, USA*
[2]*Albert Einstein Center for Fundamental Physics, Laboratory for High Energy Physics, University of Bern, Sidlerstrasse 5, CH-3012 Bern, Switzerland*
[3]*Department of Physics, Chiba University, 1-33 Yayoi-cho Inage-ku, Chiba, 263-8522, Japan*
[4]*Kyushu University, Nishi-ku, 819-0395 Fukuoka, Japan*
[5]*Department of Physics, University of Oxford, OX1 3RH, United Kingdom*
[6]*Department of Physics and Astronomy, University of Pittsburgh, Pittsburgh, PA 15217, USA*
[7]*Department of Physics and Astronomy, University of California, Irvine, CA 92697-4575, USA*
[8]*CERN, CH-1211 Geneva 23, Switzerland*
[9]*Department of Physics and Astronomy, University of California, Davis, CA 95616, USA*
[10]*Dipartimento di Fisica "E. Pancini", Università Federico II di Napoli, Napoli, Italy*
[11]*INFN Sezione di Napoli, via Cinthia, Napoli 80126, Italy*
[12]*Physics Department, Brookhaven National Laboratory, Upton, NY 11973, USA*
[13]*Department of Physics, The Ohio State University, Columbus, OH 43218, USA*
[14]*Deutsches Elektronen-Synchrotron DESY, Notkestr. 85, 22607 Hamburg, Germany*
[15]*Instrumentation Division, Brookhaven National Laboratory, Upton, NY 11973, USA*
[16]*Department of Physics & Astronomy, University of Sussex, Sussex House, Falmer, Brighton, BN1 9RH, United Kingdom*
[17]*Department of Physics and Astronomy, University of Iowa, Iowa City, IA 52242, USA*
[18]*Department of Physics and Astronomy, VU Amsterdam, 1081 HV Amsterdam, The Netherlands*
[19]*Nikhef Theory Group, Science Park 105, 1098 XG Amsterdam, The Netherlands*
[20]*Karlsruhe Institute of Technology, 76021 Karlsruhe, Germany*
[21]*Astrocent, Nicolaus Copernicus Astronomical Center Polish Academy of Sciences, ul. Rektorska 4, 00-614, Warsaw, Poland*
[22]*National Centre for Nuclear Research, Pasteura 7, 02-093 Warsaw, Poland*

High-energy collisions at the High-Luminosity Large Hadron Collider will produce a large number of particles along the beam collision axis, outside of the acceptance of existing LHC experiments. The proposed Forward Physics Facility (FPF), to be located 617–682 meters from the ATLAS interaction point along the beam collision axis and shielded by concrete and rock, will host a suite of experiments to probe Standard Model processes and search for physics beyond the Standard Model. The FPF is supported by a rapidly growing user community of 400 physicists, and four pathfinder detectors that are currently operating at the LHC have already yielded promising results, including the first direct detection of collider neutrinos. Here we provide an Executive Summary, and then briefly summarize the status of the FPF, including its rich science case, the facility itself, the proposed FPF experiments and their technical readiness, the preliminary schedule and budget profile, and plans for international participation.

Submitted to the DOE/NSF HEPAP Particle Physics Projects Prioritization Panel (P5)

CONTENTS

EXECUTIVE SUMMARY

The Forward Physics Facility (FPF) is a proposal to build a new underground cavern at the Large Hadron Collider (LHC) to host a suite of far-forward experiments during the High-Luminosity LHC (HL-LHC) era. The existing large LHC detectors have un-instrumented regions along the beam line, and so miss the physics opportunities provided by the enormous flux of particles produced in the far-forward direction. Without the FPF, the HL-LHC will be blind to neutrinos and many proposed new particles. However, small pathfinder experiments currently operating in the far-forward region at the LHC have recently directly observed collider neutrinos for the first time and demonstrated the potential for world-leading sensitivity to new physics [1–4]. With the FPF, a diverse suite of experiments will realize this potential by detecting $\sim 10^6$ neutrino interactions at the highest energies from a human source, expanding our understanding of proton and nuclear structure and the strong interactions to new regimes, clarifying astroparticle data, and carrying out world-leading searches for light dark matter, dark sectors, and many other new particles. As shown in Fig. 1, the FPF physics program spans many frontiers and will greatly enhance the LHC's physics program through to its conclusion in the 2040s.

The FPF is well aligned with the recommendations of recent community studies in the US and abroad:

- *Our highest immediate priority accelerator and project is the HL-LHC,…including the construction of auxiliary experiments that extend the reach of HL-LHC in kinematic regions uncovered by the detector upgrades.* — Snowmass 2021 Energy Frontier Report [5].

- *The full physics potential of the LHC and the HL-LHC…should be exploited.* — 1st recommendation of the 2020 European Strategy Update [6].

The FPF requires no modifications to the LHC and will support a sustainable experimental program, requiring no additional energy for the beam beyond the existing LHC program. In addition, as a mid-scale project composed of smaller experiments that can be realized on short and flexible timescales, the FPF will provide a multitude of scientific and leadership oppor-

FIG. 1. The rich physics program at the FPF spans many topics and many frontiers.

tunities for junior researchers, who can make important contributions from construction to data analysis in a single graduate student lifetime.

The Facility An extensive site selection study has been conducted by the CERN Civil Engineering group. The resulting site is shown in Fig. 2. This location is shielded from the ATLAS interaction point (IP) by over 200 m of concrete and rock, providing an ideal location to search for rare processes and very weakly interacting particles. Vibration, radiation, and safety studies have shown that the FPF can be constructed independently of the LHC without interfering with LHC operations. A core sample has been taken along the location of the 88 m-deep shaft to provide information about the geological conditions, which will be used to refine plans and cost estimates. Studies of LHC-generated radiation have concluded that the facility can be safely accessed with appropriate controls during beam operations. Flexible, safe access will allow the construction and operation of FPF experiments to be independent of the LHC, greatly simplifying schedules and budgets.

The Experiments The FPF is uniquely suited to explore physics in the far-forward region because
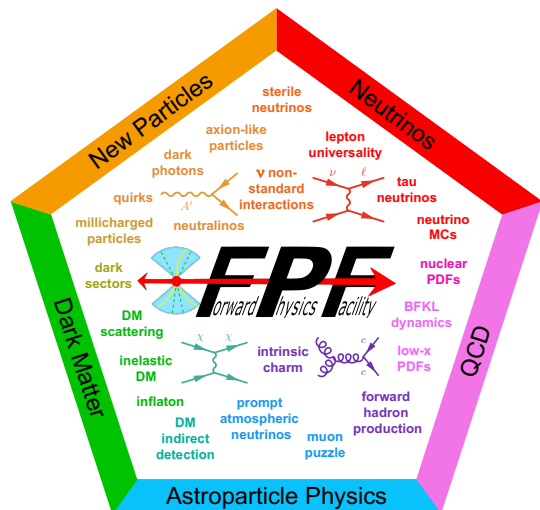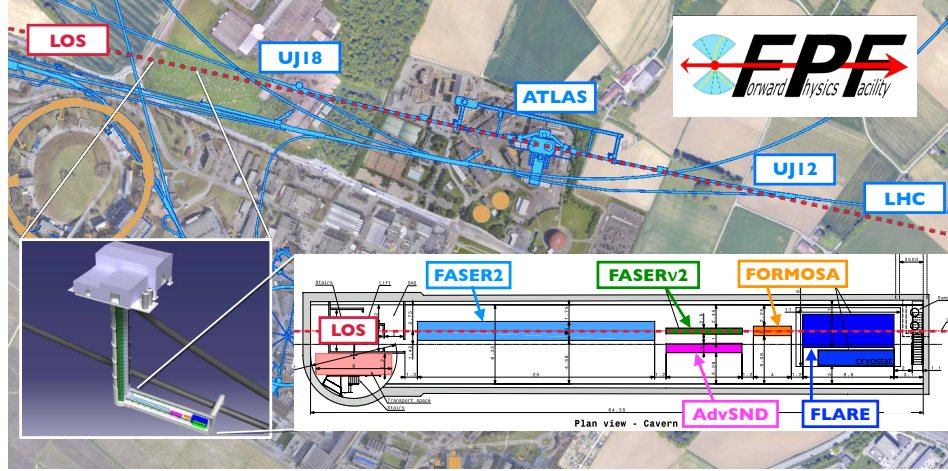
FIG. 2. The FPF location is 617–682 m west of the ATLAS IP along the beam collision axis. 65 m long and 9 m wide, the FPF cavern will house a diverse set of experiments to fully explore the far-forward region.

it will house a diverse set of experiments based on different detector technologies and optimized for particular physics goals. The proposed experiments are shown in Fig. 2 and include

- FASER2, a magnetic tracking spectrometer, designed to search for light and weakly-interacting states, including new force carriers, sterile neutrinos, axion-like particles, and dark sector particles, and to distinguish ν and $\bar{\nu}$ charged current scattering in the upstream detectors.
- FASERν2, an on-axis emulsion detector, with pseudorapidity range $\eta > 8.4$, that will detect $\sim 10^6$ neutrinos at TeV energies with unparalleled spatial resolution, including several thousands of tau neutrinos, among the least well-understood of all known particles.
- Advanced SND, an off-axis electronic detector ($7.2 < \eta < 8.4$), that will study neutrinos from charm decay and provide detailed observations of neutrino interactions for all neutrino flavors.
- FLArE, a 10-ton-scale noble liquid fine-grained time projection chamber that will detect neutrinos and search for light dark matter with high kinematic resolution and wide dynamic range.
- FORMOSA, a detector composed of scintillating bars, with world-leading sensitivity to millicharged particles across a large range of masses.

Timeline and Cost All of the planned experiments are relatively small, low cost, require limited R&D, and can be constructed in a timely way. To fully exploit the far-forward physics opportunities, many of which will disappear for several decades if not explored at the FPF, the FPF and its experiments should be ready for physics in the HL-LHC era as early as possible in Run 4. A possible timeline is for the FPF to be built during Long Shutdown 3 from 2026-28, the support services and experiments to be installed starting in 2029, and the experiments to begin taking data not long after the beginning of Run 4. Such a timeline is guaranteed to produce exciting physics results through studies of very high-energy neutrinos, QCD, and other SM topics, and will additionally enhance the LHC's potential for groundbreaking discoveries for many years to come.

A preliminary cost estimate for the facility by the CERN engineering and technical teams is $\sim$25 MCHF for the construction of the new shaft and cavern and $\sim$10 MCHF for all necessary services. Cost estimates for the experiments roughly separate into US-based costs in the range $52-83M to support the US-led experiments FLArE and FORMOSA and the US contribution to FASER2, and non-US contributions to support FASER2, FASERν2, and Advanced SND. All of the experiments will be supported by an international collaboration, however, and as the physics program begins in LHC Run 4 from 2029-32, the FPF is likely to attract a large and diverse global community.

I. SCIENCE CASE

The science case for the FPF has been developed in five dedicated FPF meetings [7–11] and through numerous Snowmass meetings, primarily in the Energy, Neutrino Physics, Rare Processes and Precision, Cosmic, and Theory Frontiers [12]. The opportunities have been summarized in a 80-page review [13] and a more comprehensive 430-page Snowmass White Paper [14], written and endorsed by 400 physicists. Here we provide a brief summary of some of the physics topics, beginning with searches for physics beyond the Standard Model (BSM), and then moving to Standard Model (SM) topics.

A. Searches for New Physics

While traditional searches for BSM physics at the LHC focus on heavy and relatively strongly interacting states, new particles might also be light, but very weakly interacting. Such light, feebly-interacting particles indeed naturally appear in many models of new physics designed to address the most significant outstanding questions in particle physics, including the nature of dark matter (DM), the electroweak hierarchy problem, the matter-antimatter asymmetry, the origin of neutrino masses, inflation, and the strong CP problem. At the LHC, such particles may be produced abundantly in the forward direction, producing a collimated beam of new particles directed at the FPF.

As illustrated in Fig. 3, the FPF BSM program encompasses a broad set of searches for novel signatures that leverages the diverse capabilities of the suite of FPF experiments. These include long-lived-particle decays to a variety of visible final states [15], DM scattering signatures [16], and unconventional ionization caused by new particles with fractional electric charge [17]. At the FPF, the precision physics program in high-energy neutrinos will open additional windows on BSM physics by probing their non-standard interactions (NSI) and oscillations into sterile neutrinos.
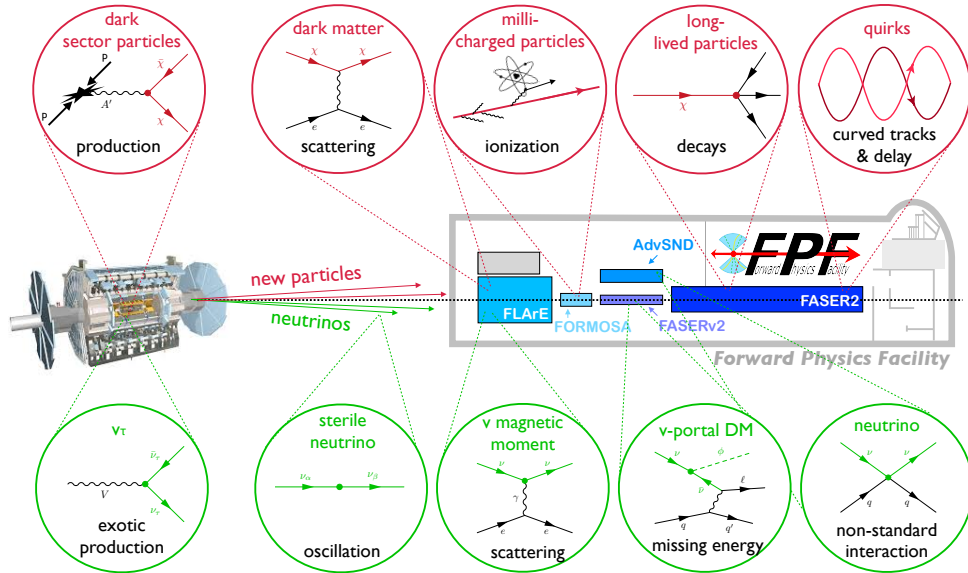

FIG. 3. **BSM Physics at the FPF.** Examples of new physics associated with dark sector particles and high-energy neutrinos that can be discovered at the FPF.
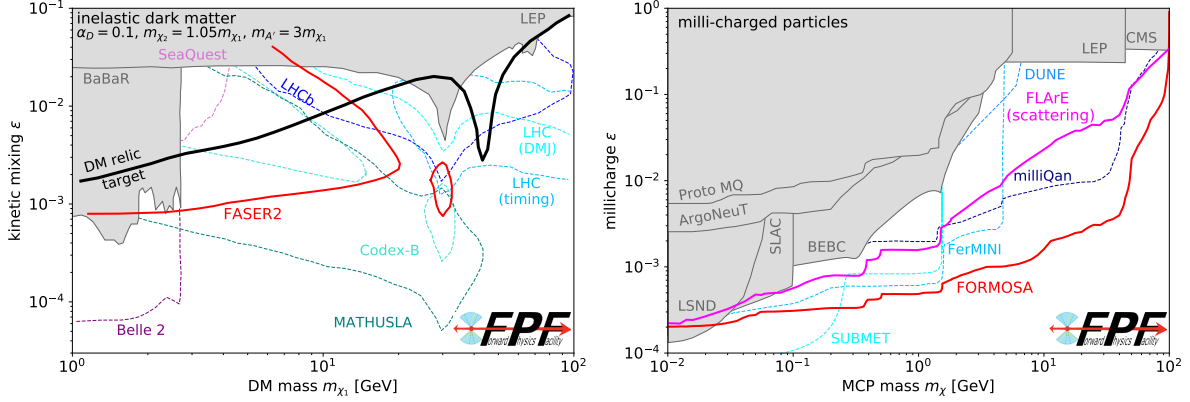
FIG. 4. **Examples of FPF Sensitivity to BSM Physics.** Left: The reach of FASER2 in the search for inelastic dark matter [18]. The thermal relic target line is marked with black solid line. Right: The reach of FORMOSA and FLArE in the search for millicharged particles [17, 19].

As noted above, comprehensive discussions of the prospects for the FPF to discover new physics can be found in Refs. [13, 14]. Two examples are shown in Fig. 4. In the left panel, the expected sensitivity of FASER2 to inelastic DM is shown for the example benchmark scenario indicated in the figure [18]. The search is focused on displaced semi-visible decays of highly-boosted excited DM states produced in pp collisions at the LHC. As can be seen, FASER2 will be able to decisively test a broad swath of parameter space where DM is produced in the early universe through thermal freezeout. Notably, the high energies available at the LHC allow for probes of larger dark sector masses than in beam-dump searches, while sensitivity to highly-displaced decays leads to a sensitivity reach that is complementary to the existing large-scale LHC detectors.

The prospects for millicharged particle (mCP) searches are shown in the right panel of Fig. 4. Such particles provide an interesting BSM physics target, both for their possible implications for the principle of charge quantization and as a candidate for a strongly interacting sub-component of dark matter. FORMOSA, a proposed scintillator-based experiment at the FPF, will have world-leading sensitivity to mCPs [17]. As seen in Fig. 4 (right panel), when compared to existing bounds and projections from several other ongoing or proposed experiments, FORMOSA benefits from the high-energy LHC collisions and the enhanced mCP production in the forward region, enabling potentially the most sensitive probe of mCPs in the broad mass range from 100 MeV to 100 GeV.

This small sampling of benchmark studies provides a few examples of the exciting BSM physics opportunities at the FPF, which will greatly expand the existing experimental program of the experiments currently operating at the LHC and elsewhere. The many experimental signatures and large range of BSM particle masses that can be probed at the FPF, from MeV up to even a few hundred GeV, provides the foundation for a broad BSM physics program that will address fundamental questions in particle physics in a manner that is complementary to other existing and proposed facilities.

B.   Standard Model Physics

The LHC is the highest energy particle collider built to date and it is therefore also the source of the most energetic neutrinos created in a controlled laboratory environment. Indeed, the LHC produces intense, strongly collimated, and highly energetic beams of both neutrinos and anti-neutrinos and all three flavors in the forward direction. Although this has been known since the
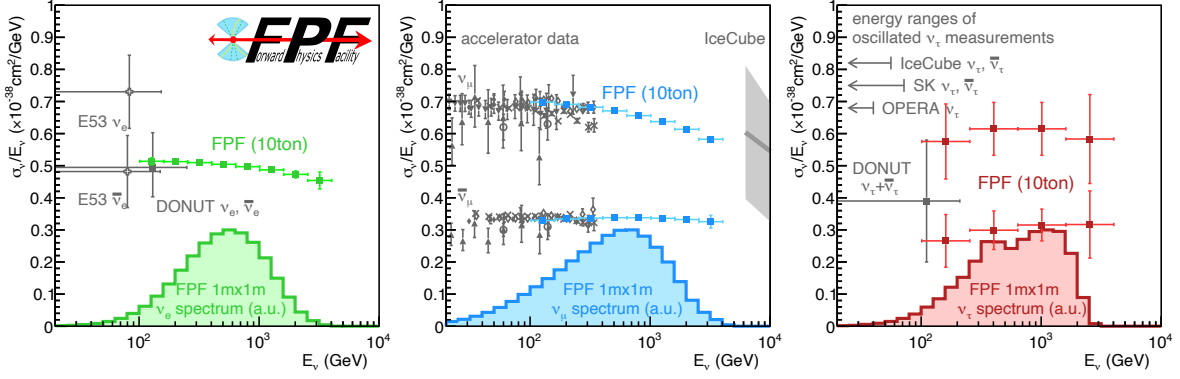
2

FIG. 5. **Neutrinos at the FPF.** The neutrino flux as a function of energy for electron neutrinos (left), muon neutrinos (middle), and tau neutrinos (right) through a $1\,\mathrm{m} \times 1\,\mathrm{m}$ area at the FPF. Also shown is the expected precision of FPF measurements of the neutrino interaction cross section with nucleons, showing statistical errors only. Existing data are shown from a compilation of accelerator experiments [20] and IceCube [21].

1980s [22], only recently have two detectors, FASERν [23] and SND@LHC [24], been installed to take advantage of this opportunity. These pathfinder experiments have just recently directly observed collider neutrinos for the first time [1–3]. By the end of LHC Run 3 in 2025, these experiments are expected to detect approximately 10^4 neutrinos. The FPF experiments, with larger detectors and higher luminosities, are projected to detect 10^5 electron neutrino, 10^6 muon neutrino, and 10^4 tau neutrino interactions, providing approximately 100 times more statistics over the installed experiments, enabling precision measurements for all three flavors, and distinguishing tau neutrinos and tau anti-neutrinos for the first time.

Fig. 5 displays the measured neutrino-nucleon charged current scattering cross sections for all three neutrino flavors. The low-energy region has been well-constrained by neutrino experiments using existing accelerators [20]. IceCube has also placed constraints on the muon neutrino cross section at very high energies using atmospheric neutrinos, although with relatively large uncertainties [21]. The histograms at the bottom of each panel show the expected energy spectra of interacting neutrinos at the FPF, which peaks at $\sim$ TeV energies, where currently no measurements exist.

Taking into account the projected statistical precision for the inclusive cross section, the FPF will enable improved calculations of neutrino scattering rates, a prerequisite for searching for, e.g., anomalous neutrino interactions in the TeV range, and validate cross section predictions required in neutrino oscillation analyses, such as those carried out at KM3NeT and IceCube. Indeed, precision SM calculations of neutrino cross sections make possible unique tests of neutrino interactions at the TeV scale, and the FPF will be able to test their flavor universality across all three generations, thanks to a large sample of 10^4 tau neutrinos.

The left panel of Fig. 6 displays the predicted number of electron neutrino interactions in the FLArE detector. The baseline prediction is represented by the gray line, with the tiny black error bars showing the corresponding statistical uncertainties. The neutrino beam is generated through the decays of pions, kaons, and charmed hadrons. Therefore, measuring the neutrino flux is a valuable method to probe hadron production in the forward region and provides insights into the underlying physics that cannot be obtained otherwise. The colored dashed lines in the figure illustrate this using three example scenarios:

- Over more than two decades, cosmic ray experiments have reported significant discrepancies
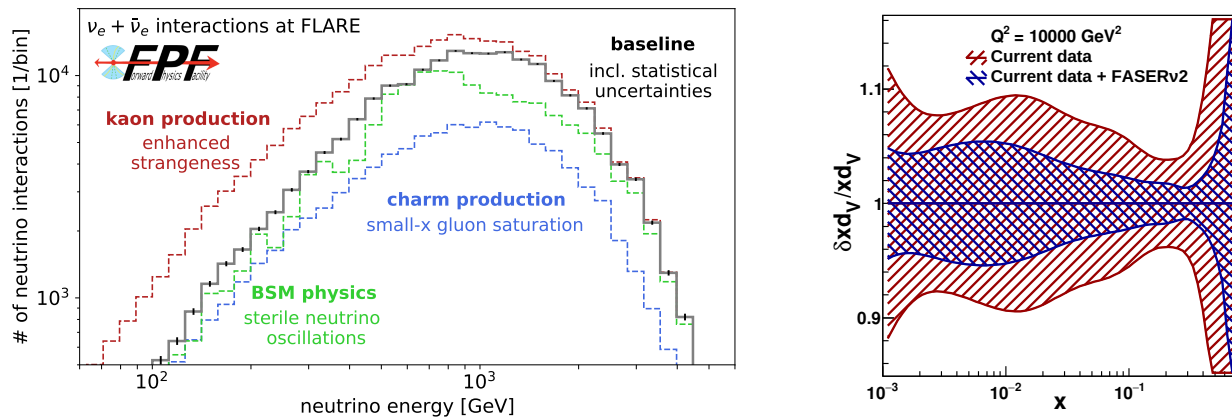
FIG. 6. **QCD at the FPF.** Left: The expected energy spectrum of interacting electron neutrinos in the FLArE detector is shown as the solid gray line. The corresponding statistical uncertainties are shown as black error bars. The colored dashed lines illustrate three examples of physics that can change the expected flux, all of which can be probed at the FPF. Right: The projected impact of the FASERν2 structure function measurements on the down quark valence PDF from the PDF4LHC21 set.

between the number of observed muons in high-energy cosmic ray air showers and model predictions [25–28]. This observation is commonly referred to as the muon puzzle. Extensive studies have suggested that an enhanced rate of strangeness production in the forward direction could explain the discrepancy [29–31]. Such scenarios can be tested at the FPF, since the the ratio of the low-energy electron and muon neutrino fluxes is a proxy for the charged kaon to pion production rate. A specific model that can resolve the muon puzzle has been proposed and studied in Ref. [32]. As shown via the red line, it predicts a significant increase of electron neutrinos with energies below 1 TeV.

- Neutrinos at high energies above 1 TeV are mainly produced in charm hadron decays. The production of charm quarks is dominated by gluon fusion and can be described using perturbative QCD. Measurements of the neutrino flux at the FPF therefore provide access to both the very high-x and the very low-x regions of the colliding protons. The former regime provides information about open questions related to the high-x parton distribution functions (PDFs) and, in particular, intrinsic charm. The latter regime is sensitive to novel QCD production mechanisms, such as BFKL effects and non-linear dynamics, as well as the gluon PDF down to $x \sim 10^{-7}$, well beyond the coverage of other experiments and providing key inputs for astroparticle physics. A specific example of physics that is expected to appear is gluon saturation. This effect causes a suppression of the gluon density at low-x and leads to a reduced flux of TeV-energy neutrinos at the FPF, as illustrated by the blue line. In addition, charm hadron decays in extensive air showers produce the main background in searches for high-energy astrophysical neutrinos. Measurements at the FPF will, therefore, also reduce the associated uncertainties of current measurements with IceCube and KM3NeT, as well as for future detectors, such as IceCube-Gen2 [33].

- The neutrino flux at the FPF is also sensitive to oscillations. For the energy and baseline of the FPF, no oscillations are expected in the SM, but the FPF can act as a short baseline neutrino experiment. The effect of electron neutrino disappearance due to an additional sterile neutrino with a mass splitting of $\Delta m^2 = 2500$ eV^2 is shown as the green line. The FPF may therefore test some of the sterile neutrino parameter space that explains the gallium anomaly [34].

In addition, the FPF acts as a neutrino-induced deep-inelastic scattering (DIS) experiment with

TeV-scale neutrino beams. Both in terms of kinematic coverage and of event statistics, the FPF will provide a window on the charged-current equivalent of the electron-proton and electron-nucleon scattering that will be observed at the upcoming EIC [35, 36]. The EIC is dominated by neutral-current events, and hence the FPF is a fully complementary probe of the quark flavor decomposition of protons and nuclei. As compared to existing DIS data on nuclear targets [37, 38], the FPF will extend the coverage in the (x, Q^2) plane by an order of magnitude in both directions [13, 14].

The right panel of Fig. 6 quantifies the projected impact of the FASERν2 muon neutrino structure function measurements on the PDF4LHC21 NNLO set [39]. Only statistical uncertainties are considered in these projections, and nuclear effects are neglected. A reduction of the proton PDF uncertainties for the valence quark distributions of up to 50% is obtained. The improved knowledge of (nuclear) PDFs made possible by FPF neutrino DIS measurements will enhance robust searches for BSM physics at the HL-LHC, for example, via the high-mass Drell-Yan process [40], and reduce theory systematics in key SM measurements such as the W boson mass [41], complementing in-situ LHC constraints [42].

II. THE FACILITY

The FPF facility has been studied in detail by a dedicated working group in the CERN Physics Beyond Collider study group. This work benefits from the huge experience at CERN related to the design and construction of large underground experimental areas, as well as operating experiments in these locations. The status of technical studies of the facility is briefly summarized in this section. More details are available in Sec. 2 of Ref. [14], and more recent studies are documented in Ref. [43].

Several possible locations for the facility around the ATLAS and CMS IPs were studied by the CERN civil engineering team. After taking into account technical, scientific, and resource considerations, it was decided to focus on a dedicated standalone new cavern situated 617 m to the west of the ATLAS interaction point (IP1). The site is in France, on land owned by CERN. As shown in Fig. 7, the facility is made up of a dedicated access shaft 88 m deep, connected to a cavern that is 65 m long, about 9 m wide/high, and centered on the collision axis line-of-sight (LOS). The dimensions of the cavern were defined based on the requirements of the proposed FPF experiments. There is at least 10 m of rock between the cavern and the LHC tunnel, which minimizes radiation and beam-related backgrounds in the facility and is also needed to ensure that the LHC tunnel will not be affected during the excavation of the FPF cavern. Preliminary studies indicate that civil engineering work to excavate the FPF cavern could be carried out during LHC operations and the vibrations from the excavation would not limit the LHC performance, and further studies are ongoing.

A very preliminary study of the needed infrastructure and services has been carried out. This includes the electrical installation, ventilation system, access and safety systems, and transport and heavy handling infrastructure. The current Class 4 [44] costing of the civil engineering work will be revised following a site investigation study that is currently underway. This involves the drilling of, and geological analysis of, a 20 cm-diameter core down to the level of the FPF cavern at the proposed location of the FPF shaft. Fig. 8 shows the ongoing site investigation works.

The CERN Sources, Targets and Interactions (STI) group has run detailed FLUKA [45–47] simulations to estimate the expected fluence of muons in the FPF, which will form the primary background for the FPF experiments. These simulations include a detailed description of the accelerator components around IP1, and predict a flux of 0.6 Hz/cm^2 around the LOS, with a significantly higher flux in some regions in the FPF more than a meter from the LOS, as can be
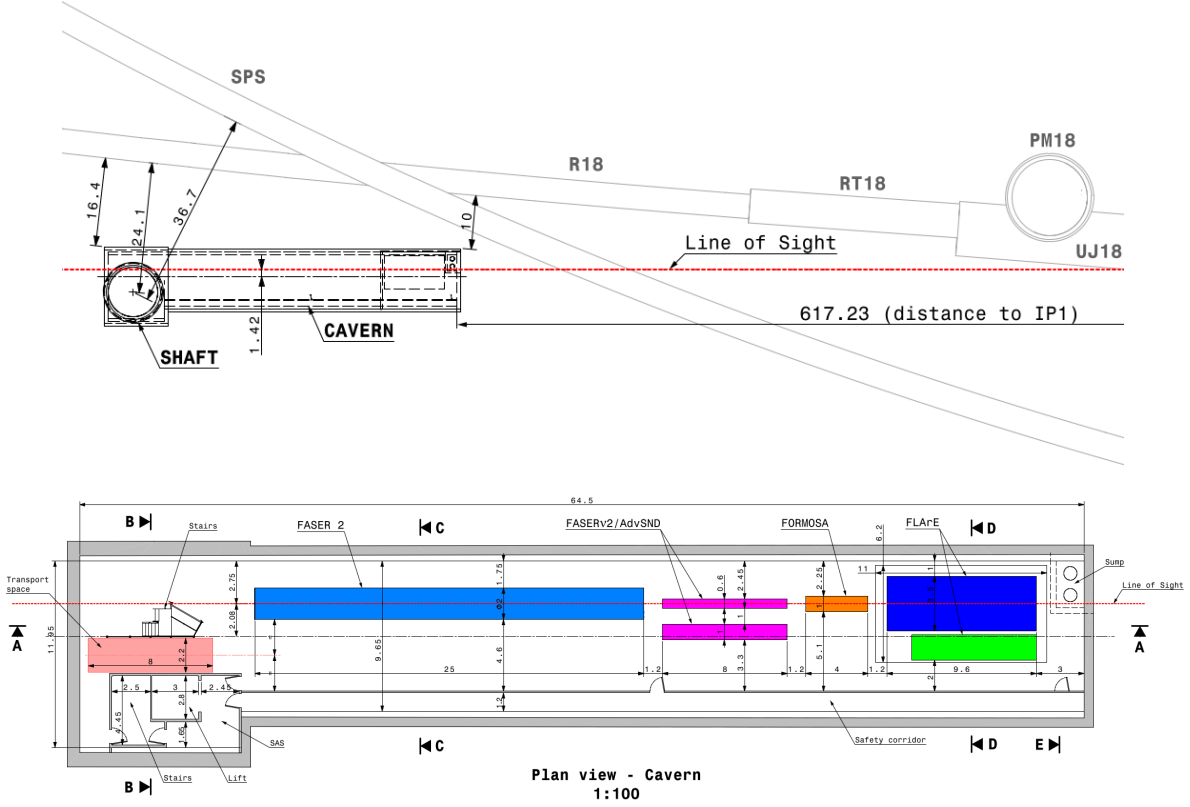
FIG. 7. Top: A plan view of the FPF shaft, which is 88 m deep, and cavern, which is 65 m long and around 9 m wide/high. Also shown is the LHC tunnel (R18, RT18), which is at the same elevation as the FPF and separated by at least 10 m of rock, and the SPS tunnel, which closer to the surface, 30 m above the FPF cavern. Bottom: A plan view of the FPF cavern, showing the location of the proposed experiments as colored blocks.

seen in Fig. 9 [43]. FLUKA simulations of the muon flux for the Run 3 LHC setup have been validated at the $\mathcal{O}(30\%)$ level with measurements by the FASER and SND@LHC experiments. FLUKA simulations have also been used to assess a possible reduction of the muon fluence by installing a sweeper magnet in the LHC tunnel about 350 m from IP1. Initial studies have not found an effective design, but studies are ongoing.

The radiation level expected in the FPF cavern has been studied by the CERN radio-protection team, based on FLUKA simulations. These studies show that the expected radiation levels will be sufficiently low to allow personnel to work in the cavern during operation of the LHC, as long as the workers are classified as radiation workers [43]. This is very important, as it implies maximum schedule flexibility and that installation, commissioning, and maintenance of the experiments will be possible during LHC operations. The expected radiation levels will also allow the use of non-radiation-hard electronics in the detector systems.

III. EXPERIMENTS AND TECHNICAL READINESS

At present, five experiments are being proposed for the FPF. Two of the five, FLArE and FORMOSA, are being developed with US leadership, and one, FASER2, is being developed by a community with US participation. The other two proposed experiments, FASERν2 and Advanced

FIG. 8. Photo of the ongoing drilling of a core at the proposed FPF location to assess the geological conditions.

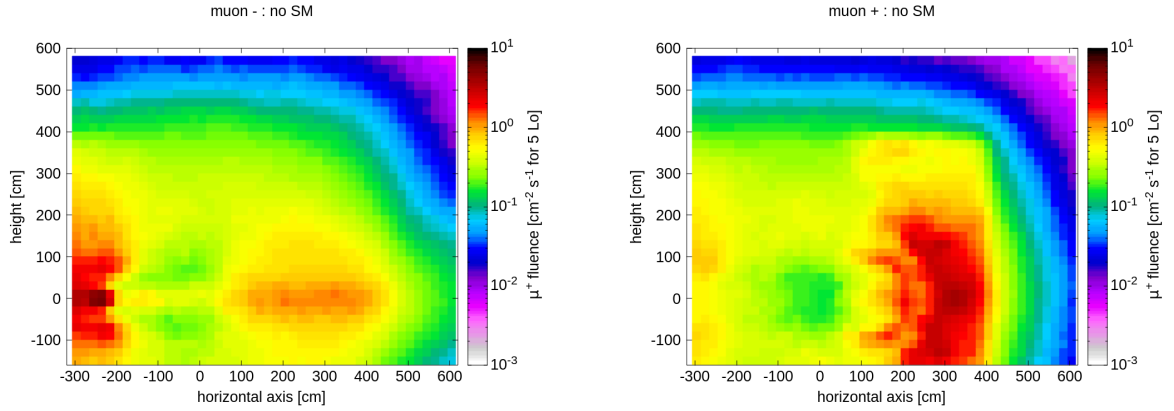

FIG. 9. The FLUKA estimate of the muon fluence at the FPF for the nominal HL-LHC luminosity of 5×10^{34} cm^{-2} s^{-1} for negative muons (left) and positive muons (right).

SND, do not currently have strong US participation. Here we describe all five of the experiments. The construction schedule and breakdown of costs is discussed below in Sec. IV.

A. FASER2

FASER2 is a large-volume detector comprised of a spectrometer, electromagentic and hadronic calorimeters, veto detectors, and a muon detector. FASER2 is designed for sensitivity to a wide variety of models of BSM physics and for precise muon reconstruction. It builds on positive experience gained from the successful operation of the existing FASER detector [48], a much smaller detector that is constrained to lie within a LHC transfer tunnel. The FASER2 detector, which is designed for the FPF facility, is much larger (by a factor of ~ 600 in decay volume size) and includes new detector elements. It has an increase in reach for various BSM signals of several orders of magnitude compared to FASER and allows sensitivity to particles that were previously out of reach, such as dark Higgs bosons, heavy neutral leptons, and some axion-like particles, as studied in Refs. [15, 23, 49]. In addition to the BSM case for FASER2, the SM neutrino program at the FPF will rely on the identification of muons from neutrino decays and precise measurement of their momentum and charge. The FASER2 spectrometer will be integral for these measurements for both FASERν2 and FLArE.

To enable realistic detector design studies, a Geant4 geometry of the proposed detector has been created; a diagram is shown in Fig. 10. The overall FASER2 design is largely driven by the spectrometer with further consideration having been given to deliverable and affordable magnet technology leading to a split spectrometer with a large-volume dipole magnet. The magnet has a rectangular aperture of 1 m in height and 3 m in width. This also defines the transverse size of decay volume, which is the 10 m un-instrumented region upstream of the first tracking station (a $3 \times 1 \times 10$ m^3 cuboid) and downstream of the first veto station. The transverse size is driven by the need to have sufficient sensitivity to BSM particles originating from heavy flavor decays.

The baseline magnetic field is one with 4 Tm of bending power. This field strength is required to achieve sufficient particle separation, momentum resolution, and charge ID performance for the BSM and neutrino program. Superconducting magnet technology is required to maintain such a field strength across a large aperture. Technology based on the magnet of the SAMURAI experiment [50] is currently being pursued. The tracking detectors are foreseen to use a SiPM and scintillating fiber tracker technology, based on LHCb's SciFi detector [51]. This technology gives sufficient spatial resolution (~ 100 μm) at a significantly reduced cost compared to silicon detectors. However, the use of silicon-based tracking detectors will be explored for the interface between FASER2 and FASERν2, and for the first tracking station downstream of the decay volume.

The calorimeter is foreseen to be based on dual-readout calorimetry [52, 53] technology, building from experience of existing prototypes for future collider R&D, but modified for the specific physics
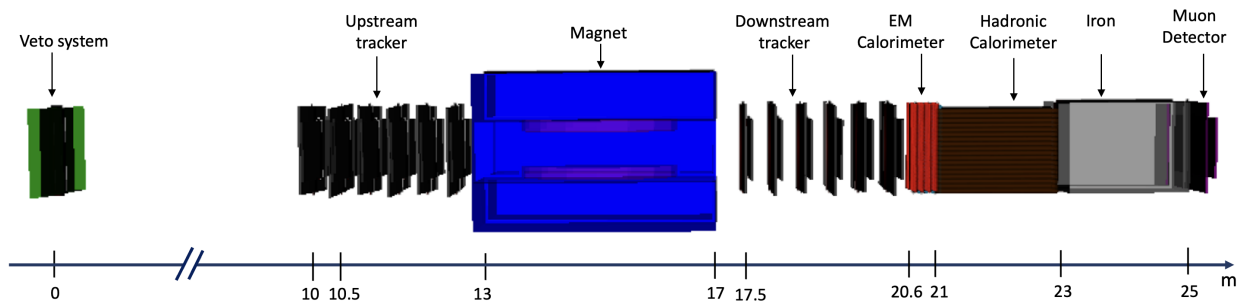

FIG. 10. Schematic diagram of the full FASER2 detector, showing the veto system, un-instrumented 10 m decay volume, tracker, magnet, electromagnetic calorimeter, hadronic calorimeter, iron absorber, and muon detector.

needs of FASER2: spatial resolution to be able to identify particles at $\sim 1-10$ mm separation; good energy resolution; improved longitudinal segmentation with respect to FASER; and the capability to perform particle identification, separating, for example, electrons and pions. The ability to identify separately electrons and muons will be very important for signal characterization, background suppression, and for the interface with FASERν2. To achieve this, a mass of iron will be placed after the calorimeter, with sufficient depth to absorb pions and other hadrons, followed by a detector for muon identification, for which additional SciFi planes could be used.

Finally, the veto system will be required to reject muon rates of approximately 20 kHz. Scintillator-based approaches have proven to be sufficient for this in FASER, and a similar, but re-optimised, design is foreseen for FASER2. The event rate and size are much lower than most LHC experiments, so the trigger needs are not expected to be a limiting issue. For instance, it is expected that it will be possible to significantly simplify the readout of the tracker, with respect to what is used in the LHCb SciFi detector.

B.   FASERν2

FASERν2 is a 20-ton neutrino detector located on the LOS, a much larger successor to the FASERν [54, 55] subdetector in the FASER experiment. An emulsion-based detector will identify heavy flavor particles produced in neutrino interactions, including tau leptons and charm and beauty particles. FASERν2 can perform precision tau neutrino measurements and heavy flavor physics studies, testing lepton universality in neutrino scattering and new physics effects, as well as providing important input to QCD and astroparticle physics, as described in Sec. I.

Fig. 11 shows a schematic of the proposed FASERν2 detector, which is composed of 3300 emulsion layers interleaved with 2-mm-thick tungsten plates. The total volume of the tungsten target is 40 cm $\times$ 40 cm $\times$ 6.6 m, with a mass of 20 tons. The detector will be placed directly in front of the FASER2 spectrometer along the LOS. The FASERν2 detector will also include a veto system and interface detectors to the FASER2 spectrometer, with one interface detector in the middle of the emulsion modules and the other detector downstream of the emulsion modules. These additional systems will enable a FASER2-FASERν2 global analysis and make measurement of the muon charge possible, a prerequisite for $\nu_\tau/\bar{\nu}_\tau$ separation. The veto system will be scintillator-based, and the interface detectors could be based on silicon strip sensors or scintillating fiber tracker technology. The detector length, including the emulsion films and interface detectors, will be approximately 8 m.

As the $c\tau$ of the tau lepton is 87 μm, a high-precision emulsion detector is essential to detect tau decays topologically. After optimizations of the detector performance (in terms of precision, sensitivity, and long-term stability), we will use an emulsion gel with silver bromide crystals of 200 nm diameter and a volume occupancy of 35%, which provides an intrinsic position resolution of 50 nm. The emulsion detector will be placed in a cooling box and kept at around 10° C to avoid fading of the recorded signal. Emulsion detector analysis is limited by the accumulated track density and becomes very difficult above 10^6 tracks/cm^2. To keep the accumulated track density at an analyzable level, the emulsion films will be replaced once per year, with a total of 520 m^2 of emulsion film used annually. The implementation of an effective sweeper magnet to reduce the muon fluence in the FPF would be very beneficial for the FASERν2 experiment, and studies on possible designs for this are ongoing.

The emulsion film production and its readout will be conducted at facilities in Japan. The capacity of the film production facility is 1200 m^2 per year. The HTS scanning system can read out $\sim$0.5 m^2 per hour, or 1,000 m^2 per year. Analysis methodologies dedicated to TeV-neutrinos
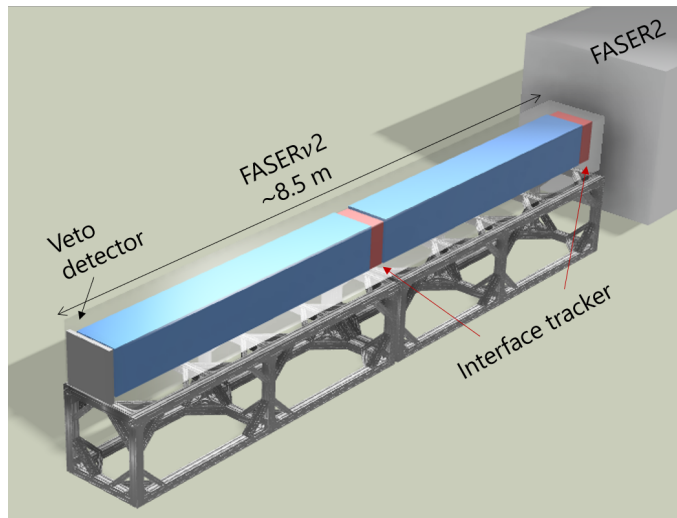
FIG. 11. Conceptual design of the FASERν2 detector.

are currently being developed and tested for the FASERν experiment. These methods include momentum measurements using multiple Coulomb scattering information, electromagnetic shower reconstruction, and machine learning algorithms for neutrino energy reconstruction.

FASERν2 has a clear and broad physics target, and the detector is based on a well-tested technology for tau neutrino and short-lived particle detection. Further studies will be carried out to optimize the detector performance, the detector operational environment, and the installation scheme.

C. Advanced SND

The Advanced SND project will extend the physics case of the SND@LHC experiment [24]. It will consist of two detectors: one placed in the same range of pseudorapidity η as SND@LHC, i.e., $7.2 < \eta < 8.4$, hereafter called FAR, and the other one in the region $4 < \eta < 5$, hereafter denoted NEAR. The FPF can host the FAR detector. The NEAR detector, given the higher average angle, would have to be placed more upstream to have a sizeable azimuthal angle coverage.

Here we concentrate on the FAR detector. A schematic view of the detector is given in Fig. 12. It will be made of three elements. The upstream one is the target region for the vertex reconstruction and the electromagnetic energy measurement with a calorimetric approach. It will be followed downstream by a hadronic calorimeter and a muon identification system. The third and most downstream element will be a magnet for muon charge and momentum measurement, thus allowing for neutrino/anti-neutrino separation for muon neutrinos and for tau neutrinos in the muonic decay channel of the tau lepton.

The target will be made of thin sensitive layers interleaved with tungsten plates, for a total mass of ~ 5 tons. The use of nuclear emulsion requires frequent replacement, given the very high luminosity of the HL-LHC. The Collaboration is therefore investigating the use of compact electronic trackers with high spatial resolution, fulfilling both the tasks of vertex reconstruction with micrometer accuracy and electromagnetic energy measurement. The hadronic calorimeter and the muon identification system will have a length of about 10λ, where λ is the nuclear interaction length, which will bring the average length of the hadronic calorimeter to about 12λ, thus improving the
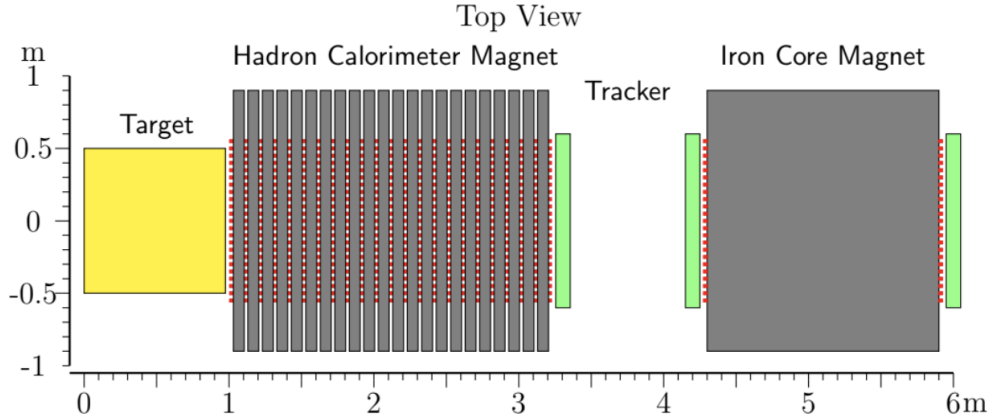
FIG. 12. Layout of the Advanced SND – FAR detector proposed for the FPF.

muon identification efficiency and energy resolution.

The magnet is a key element in the detector design because it will make it possible to measure the lepton number of muon neutrinos and of tau neutrinos when the tau lepton decays into a muon, by identifying the charge of the outgoing muon. To make the full detector more compact, the current design foresees an iron core magnet, with the magnetization also of the hadronic calorimeter. In this way, the muon trajectory will be bent starting from downstream of the target, thus reducing the full length of the detector. The calorimeter magnet consists of 22 iron slabs, each 8 cm-thick, with 2 cm-wide gaps. The second magnet consists of 20 iron slabs that are 8 cm-thick without any gaps. The magnetic field strength in the iron is assumed to be 1 T.

The determination of the muon momentum relies on the measurement of four coordinates: the most upstream is where the muon originates, either the primary neutrino interaction or the tau lepton decay vertex; the coordinate at the exit of the hadronic calorimeter; the coordinate at the entrance of the second magnet; and the coordinate at the exit of the second magnet. For the muon charge assignment, the maximum muon momentum, $p_{\max}$, for which a charge assignment is possible, can be defined by requiring at least a 4σ separation from infinite momentum, corresponding to a momentum resolution of $\Delta p/p = 1/4$ for $p = p_{\max}$. The detector is designed to guarantee a 4σ separation for muon momenta up to 750 GeV, assuming perfect tracker alignment.

D.   FLArE

A modularized liquid argon time projection detector (FLArE) is under development for the suite of detectors for the FPF. The technical design of such a detector is helped by the considerable investment in liquid noble gas detectors over the last decade (ICARUS, MicroBooNE, SBND, ProtoDUNE, and various components of DUNE). A liquid argon detector offers the possibility to precisely determine particle identification, track angle, and kinetic energy over a large dynamic range, from ~ 10 MeV to many hundreds of GeV. Such a broad-purpose detector is therefore complementary to other FPF detectors (such as emulsion detectors or magnetic spectrometers) that are more tuned for single-purpose measurements. The liquid argon detector is motivated by the requirements of neutrino detection [13] and light dark matter searches [16]. A key motivation is the detection and measurement of TeV-scale neutrino events from a laboratory-generated, well-characterized source: the LHC. The LHC is the only possible intense terrestrial source of high-

11

energy neutrinos. The data set that will be gathered at FLArE and other far-forward detectors will thus be unique and broadly valuable to particle physics and astrophysics.

The detector is expected to measure millions of neutrino interactions, including tau neutrinos. The detector should have sufficient capability to measure these very high-energy (> 100 GeV) events, so that the cross section for each flavor can be measured. Identification of tau neutrinos with low backgrounds requires detailed simulations and reconstruction studies. As an approximate estimate, we expect to see about 25-50 high-energy neutrino events/ton/fb^{-1} of collisions. (Note that during the high-luminosity running of the LHC, the beam delivers approximately 1 fb^{-1} per day.) The majority of this flux will be muon neutrinos, with electron neutrinos forming about 1/5 of the event rate. The tau neutrino rate is expected to be ~ 0.1 event/ton/fb^{-1}, with a very large uncertainty due to QCD modeling in the forward direction. The high-energy electron and tau neutrino fluxes come from charm meson decays in the forward region, and, therefore, careful measurements of these event types have broad implications for particle physics, as described in Sec. I.

The key requirement for both measurements, neutrinos and light dark matter, is the ability to trigger and collect particles that come from the ATLAS IP and produce an event within the fiducial volume of the detector, in the presence of large muon backgrounds from the high luminosity running of the LHC. The detector must also be able to contain the events and reconstruct the kinematics to identify the neutrino type. Identification of tau neutrinos presents a particular challenge requiring both high spatial and kinematic resolution. In the case of dark matter events, an isolated forward-going electron must be identified and its energy measured. A liquid argon (or noble liquid) time projection chamber provides the opportunity to have sub-millimeter spatial resolution in all three dimensions, along with excellent electromagnetic calorimetry. For excellent energy containment and muon tagging and measurement, the detector will need a magnetized hadron/muon calorimeter downstream of the liquid argon volume.

Table I summarizes the main parameters of a LArTPC for the FPF. A detector with a fiducial (active) mass of approximately 10 tons (30 tons) of liquid argon is envisioned. The dimensions of the TPC are preliminary. The TPC is designed to be modular for two main reasons: first, the muon rate at the FPF is sufficiently high that the space charge intensity requires a short gap (< 50 cm); and second, the trigger capability is enhanced by compartmentalizing the intense scintillation light

	Value	Remarks
LAr detector fiducial mass	>10 tons	
Active dimensions	1.8 m × 1.8 m × 7 m	not including cryostat
Cryostat dimensions	3.5 m × 3.5 m × 9.6 m	membrane type
TPC modules/drift length	3 × 7 (gap: ∼30 cm)	short gap TPC
TPC height	1.8 m	
Spatial resolution	<1 mm	in drift and tranverse dimension
Charge readout	pixels	pixel/wire hybrid approach possible
Trigger and light readout	SiPMs/WLS-plates	needed for neutrino trigger and time
Background muon rate	$\sim 1/\text{cm}^2/\text{s}$	at luminosity $5 \times 10^{34}/\text{cm}^2/\text{s}$
Neutrino event rate	$\sim 50/\text{ton}/\text{fb}^{-1}$	for all flavors of neutrinos
Hadronic calorimeter (hadmu)	$\sim 6 - 10\lambda$	interactions lengths
Dimensions	1.8 m × 1.8 m × 1.05 m (depth)	Fe/scint sandwich
Muon tagger and momentum	1 Tesla magnetized Fe/scint	same as the hadmu

TABLE I. Detector parameters for a LArTPC for the FPF. The top part of the table shows the nominal geometric parameters for the time projection chamber, and the bottom part shows the parameters for the additional hadron and muon detectors.
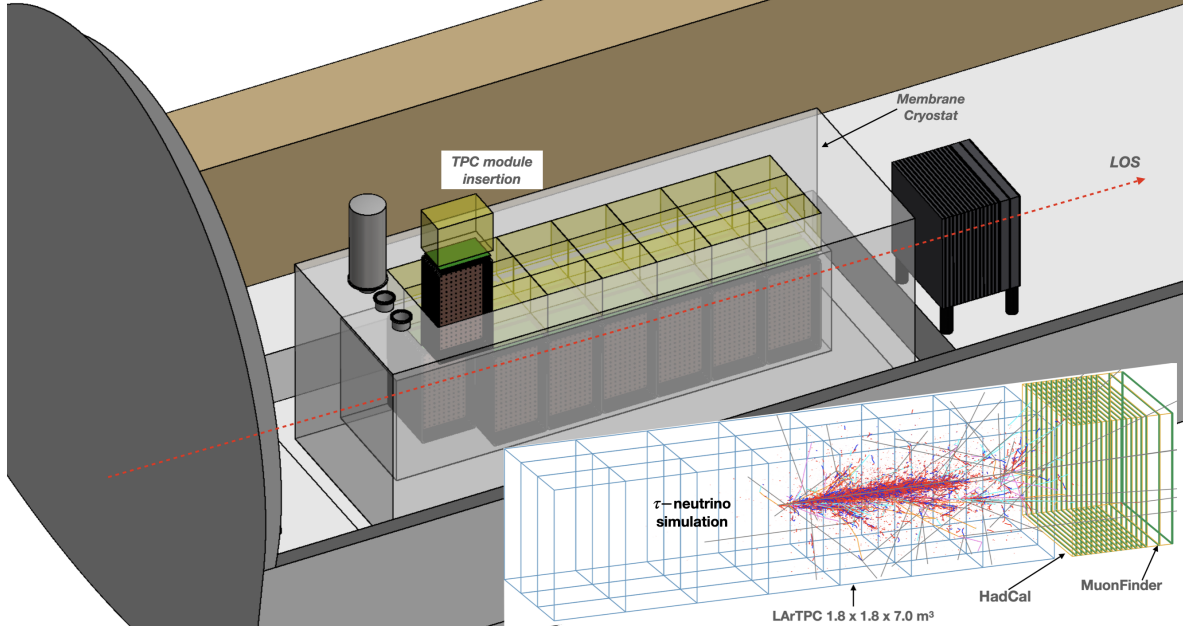
FIG. 13. Layout of FLArE detector in the FPF cavern with a simulated neutrino event inset. The detector is shown with an example of a TPC module being inserted from the top.

from liquid argon.

The main design choices for the TPC are the cryostat, TPC modules, TPC gap dimension, and overall dimensions for event containment. These have been examined by the FLArE technical group and found to be sound. Fig. 13 shows the schematic of FLArE located in the front of the FPF cavern with a simulated tau neutrino event (with energy of ~ 500 GeV) in the inset. Furthermore, the TPC dimensional choices allow low track distortion due to space charge, ease of trigger design based on modular light detection, and ease of installation in the underground hall. Two design choices will require further R&D: the TPC charge readout electronics must be re-optimized for high spatial resolution and larger dynamic range using experience from the DUNE design, and the trigger design will require detailed simulations and software development. There is sufficient time and expertise available for these tasks.

The FLArE project is divided into three major components: the needed infrastructure in the FPF cavern; the cryostat and cryogenics; and the detector, including all instrumentation, electronics, DAQ, and associated software. The costs will be divided between CERN (for the infrastructure), the US collaboration, and the non-US partners. Given that FLArE is roughly the same scale (but with a different detailed design), the recent experience with MicroBooNE and SBND at FNAL is applicable. We anticipate that the US cost estimate, $39-65 M in FY2023 dollars (exclusive of the infrastructure cost), will be kept below the threshold that allows the project to be managed by a US national laboratory with significant organizational experience at CERN and under US-DOE guidance.

The FLArE project will follow guidance and review processes as defined by the US-DOE and CERN along with other significant partners. Currently, two international working groups, the FLArE physics and technical groups, are active with large US participation. If the project is encouraged, these working groups will form a proto-collaboration with constituent bodies for scientific and technical decision-making. A large part of the collaboration function in the next two years will be defining the science and detector scope, working to coordinate with the other elements of the

FPF, and obtaining the research related resources from appropriate national funding agencies for a conceptual design and the needed R&D.

E. FORMOSA

The FPF provides an ideal location for a next-generation experiment to search for BSM particles that have an electrical charge that is a small fraction of that of the electron. Although the value of this fraction can vary over several orders of magnitude, we generically refer to these new states as "millicharged" particles (mCPs). Since these new fermions are typically not charged under QCD, and because their electromagnetic interactions are suppressed by a factor of $(Q/e)^2$, they are "feebly" interacting and naturally arise in many BSM scenarios that invoke dark or otherwise hidden sectors. For the same reason, experimental observation of mCPs requires a dedicated detector.

As proposed in Ref. [17], FORMOSA will be a milliQan-type detector [56, 57] designed to search for mCPs at the FPF. FORMOSA will be technically similar to what the milliQan Collaboration has installed in the PX56 drainage gallery near the CMS IP at LHC Point 5 for Run 3 [58], but with a significantly larger active area and a more optimal location with respect to the expected mCP flux.

To be sensitive to the small dE/dx of a particle with $Q \lesssim 0.1e$, an mCP detector must contain a sufficient amount of sensitive material in the longitudinal direction pointing to the IP. As in Ref. [56], plastic scintillator is chosen as the detection medium with the best combination of photon yield per unit length, response time, and cost. Consequently, FORMOSA is planned to be a $1 \text{ m} \times 1 \text{ m} \times 5 \text{ m}$ array of suitable plastic scintillator (e.g., Eljen EJ-200 [59] or Saint-Gobain BC-408 [60]). The array will be oriented such that the long axis points at the ATLAS IP and will be located on the LOS. The array contains four longitudinal "layers" arranged to facilitate a 4-fold coincident signal for feebly-interacting particles originating from the ATLAS IP. Each layer in turn contains 400 $5 \text{ cm} \times 5 \text{ cm} \times 100 \text{ cm}$ scintillator "bars" in a 20×20 array. To maximize sensitivity to the smallest charges, each scintillator bar is coupled to a high-gain photomultiplier tube (PMT) capable of efficiently reconstructing the waveform produced by a single photoelectron (PE). To reduce random backgrounds, mCP signal candidates will be required to have a quadruple coincidence of hits with $\overline{N}_{\text{PE}} \geq 1$ within a 20 ns time window. The PMTs must therefore measure the timing of the scintillator photon pulse with a resolution of ≤ 5 ns. The bars will be held in place by a steel frame. A conceptual design of the FORMOSA detector is shown in Fig. 14.

Although omitted for clarity in Fig. 14, additional thin scintillator "panels" placed on each side of the detector will be used to actively veto cosmic muon shower and beam halo particles. Finally, the front and back of the detector will be comprised of segmented veto panels using perpendicular scintillator bars. This will provide efficient identification and tracking of the muons resulting from LHC proton collisions through the detector. During Run 2 of the LHC, a similar experimental apparatus (the milliQan "demonstrator") was deployed in the PX56 draining gallery at LHC P5 near the CMS IP. This device was used successfully to search for mCPs, proving the feasibility of such a detector [61].

Even though the pointing, 4-layered design will be very effective at reducing background processes, small residual contributions from sources of background that mimic the signal-like quadruple coincidence signature are expected. These include overlapping dark rate pulses, cosmic muon shower particles, and beam muon afterpulses. In Ref. [58], data from the milliQan prototype was used to predict backgrounds from dark rate pulses and cosmic muon shower particles for a closely related detector design and location. Based on these studies, such backgrounds are expected to be negligible for FORMOSA. Backgrounds from muon afterpulses are considered in Ref. [17] and can
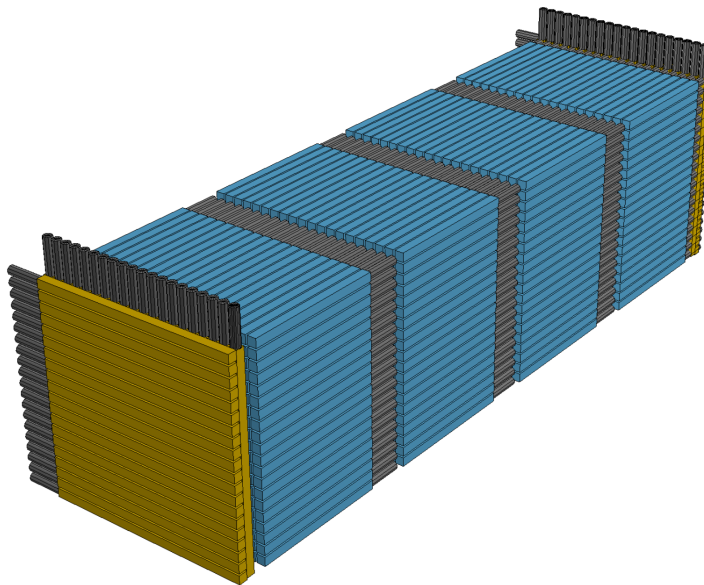
FIG. 14. A diagram of the FORMOSA detector components. The scintillator bars are shown in blue connected to PMTs in black.

be rejected by vetoing a 10 μs time window in the detector following through-going beam muons. This veto will be improved by the muon tracking provided by the segmented bars at the front and back of the detector.

The FORMOSA detector is proposed to be constructed of plastic scintillator, however, in the coming years, the exciting possibility of using alternative scintillator material with significantly higher light-yield will be studied. One such material is CeBr3 scintillator (available from Berkeley Nucleonics). This provides a light yield approximately factor 30 times higher than the same length of plastic scintillator with excellent timing resolution. This would allow much lower charges to be probed with the FORMOSA detector. Further updates to the detector design can be studied with a FORMOSA demonstrator in the forward region of the LHC.

IV. SCHEDULE AND BUDGET PROFILE

A very preliminary budget and schedule has been assembled for the FPF facility and the component experiments. The budget process was initiated at the FPF5 meeting, held 15-16 November 2022 at CERN [11]. The costs are in three separate groups, as indicated in Table II.

The cost range for the civil construction and the outfitting was provided by the CERN civil engineering group and the technical infrastructure groups, respectively. They reviewed the initial experimental requirements for the needed location, underground space, and services, and performed a Class 4 estimate [44]. According to international standards of conventional construction, a Class 4 estimate has a range of (+50% and -30%) around the point estimate. The outfitting includes electrical service, as well as safety, ventilation, transportation, and lift services that are needed for the facility. Obviously, the facility costs depend on the experimental requirements, which are expected to evolve as we progress towards a technical design.

The costs for the experimental program were assembled by proponents at the FPF5 meeting. These raw or core costs are shown in Table II for FASERν2, FASER2, and Advanced SND. The

costs for FASERν2 are dominated by production and handling of emulsion. For FASER2 and Advanced SND, the costs are dominated by the proposed magnetic spectrometer systems. The US components for these projects are currently not well defined, and therefore these core costs are provided without labor, overhead, contingency, and additional factors that must be used for a full cost estimate for US agencies.

For FASER, there is a sizable US collaboration and interest. This collaboration intends to participate fully in the FASER2 project with US funding support. The current US scope for FASER2 is uncertain, but it is clear that the project will require specialized expertise in large spectrometer magnet design, as well as tracking. This expertise can be obtained from national labs in the US and abroad. We have assumed that the preliminary scope for the US portion of FASER2 will be the design and integration of the superconducting coils needed for this magnet. The design, fabrication, underground installation, and testing of such a superconducting magnet is somewhat novel. Therefore, we envision a joint US/Japan project for this magnet, as well as integration with the spectrometer and the facility. Proposals are ongoing for such a joint project. The US FASER2 contribution has very preliminary estimates on engineering and design of these specialized coils with 50% contingency.

For FLArE and FORMOSA, which have substantial US portions, we have included our preliminary estimates for engineering, management, labor, overhead, and contingency factors to the best of our current knowledge and ability. FORMOSA is a conventional plastic scintillator-based detector with PMT readout. The estimate includes mostly off-the-shelf parts and conventional assembly. We have therefore assigned a 20% contingency to the estimate; the range corresponds to options for electronics. The FLArE estimate is based on the DUNE ND design. However, it will require targeted R&D for the TPC electronics, a sophisticated photon sensor system, trigger electronics, and clean assembly. Therefore, we have assigned a 40% contingency. These costs also include laboratory and university labor rates for FLArE and FORMOSA, respectively. Granular details for the FLArE and FORMOSA costs are available at a pre-conceptual level. These costs will be refined and further improved as we proceed to the conceptual design. A few additional comments are necessary for the US project costs:

- The range in the US estimates is not due to contingency. It is an uncertainty based on technical or management choices as we describe below. Contingency is applied on both the low and upper ends of the estimates.
- The upper limit of the FLArE costs include a GTT membrane style cryostat using the same technology as the protoDUNE and SBND detectors. This technology was developed as part of the DUNE development. The costs for FLArE were assembled using the DUNE liquid argon near detector conceptual design report as a resource. The cryostat/cryogenics cost for FLArE is approximately $12M.
- The upper limit of the FLArE cost also includes additional infrastructure costs, which are expected for the assembly and integration of FLArE into the FPF. Conservatively, we have assigned $8M including labor, based on our experience with other liquid argon projects.
- The cryostat/cryogenics and additional infrastructure design and costs clearly need to be coordinated and shared with CERN. This process of coordination has started only recently. For the purposes of this report, we have included the full estimate of these costs with contingency factors in our table under US-DOE costs for the *upper* range. *The lower range corresponds to these costs being covered under agreement with CERN.*
- The cost for the US includes labor for engineering and construction of the experiments, but does not include the research support that will be needed. Obviously, for an effort of this size, considerable support will be needed by a collaboration for students, postdocs, travel, and R&D.

Component	Cost Range	Comments
Facility Costs		
FPF civil construction	20-35 MCHF	Construction of shaft and cavern
FPF outfitting costs	7-15 MCHF	Electrical, safety, and other services
Total	**27-50 MCHF**	Total including integration
Int'l Experiment Costs		Labor, overhead, contingency not included
FASER2	17 MCHF	Non-US portion
FASERν2	16 MCHF	
ADV-SND	12 MCHF	
Total	**45 MCHF**	
US Experiment Costs		Labor, overhead, contingency included
FLArE	$39-65 M	Contingency 40%
FORMOSA	$7-8 M	Contingency 20%
FASER2	$6-10.5 M	Contingency 50%, US portion
Total	**$52-83.5 M**	

TABLE II. Cost ranges for components of the FPF and the experimental program. Costs of the infrastructure at CERN are Class 4 estimates according to international standards; they have a range ($+50\%$ and -30%). The costs for experimental components other than FLArE and FORMOSA are estimated as core costs, which consist of direct costs of materials and contracts only. The US costs include the costs for FLArE, FORMOSA, and portions of FASER2 appropriate for the US. The US costs include engineering and labor rates from either US laboratories or universities and include contingency (see text). Escalation over the construction period was added for US costs also. As described in the text the cost ranges result from technical or management choices that will be made in the future. All cost ranges are in FY2023 dollars.

This is not included in the table. We estimate the US size of the collaboration to range from 100 to 200 people with annual support at the scale of $\sim$ $5–10M.

The cost estimate for the FPF and its experiments will be refined in successive stages and reviews as normally done for large MIE (Major Item of Equipment) acquisitions. We expect the review process to be defined by CERN as the host lab, and the leading funding organizations, for the US side, by the US-DOE. Clearly, additional steps are needed to better define the scope of the facility and the constituent physics experiments. The FPF community will continue with its working group activities and the FPF workshops. Detailed simulation activities have commenced and have provided critical information on detector size and depth needed for good efficiency and energy containment for various types of neutrino interactions, as well as for sensitive searches for the many possible BSM scenarios. The CERN accelerator and radiation safety groups have contributed immensely by providing detailed simulations of the muon rates. These simulation activities will require appropriate levels of support to develop the detailed requirements needed for a conceptual design report.

The overall physics output from the FPF may be maximized by combining information from the different experiments. Some thought has gone into the layout of the facility to allow this; this will be further explored as the experiment designs become more mature. We anticipate that a detailed conceptual design report with the next level of coordination among the experimental projects and better scope definition for the facility will be completed in 2024/2025.

Table III has the proposed funding profile using the current understanding of the cost estimates for the US-DOE components. In the following we provide the constraints used for assembling this funding profile:

- Table III includes some milestones and the nominal HL-LHC schedule. Any FPF construction must be coordinated with the HL-LHC, so that the civil construction and demands on personnel

Year	2022	2023	2024	2025	2026	2027	2028	2029	2030	2031	2032	2033-34
(HL)-LHC nominal schedule	Run3	Run3	Run3	Run3	LS3	LS3	LS3	Run4	Run4	Run4	Run4	LS4
FPF/FLARE milestones		Pre-CDR and physics proposal	R&D and detetor prototypes	CDR- long lead item magnet	Start of civil constr. TDR for detectors	Detector construction start	Long lead items for detector	End of civil constr. Install services	Detector install	Detector Commissioning and physics start	Physics running with full complement of detectors	
US-DOE FLARE (kUS$)						9750	19500	19500	13000	3250		
US-DOE FORMOSA (kUS$)						800	1600	4000	1600			
US-DOE-FASER2 (kUS$)			875	1750	3500	2625	1750					
Total US-DOE (kUS$)			875	1750	3500	13175	22850	23500	14600	3250		

TABLE III. Proposed funding profile for the US DOE portion of the FPF experimental program using the upper ranges from Table II. The main components are FLArE, FORMOSA, and US contributions to FASER2. The estimates include all technical components and laboratory and university labor with appropriate overhead factors. The FLArE estimate has a 40% contingency applied, and the FORMOSA estimate has a 20% contingency applied. Cost numbers are in FY2023 dollars.

do not interfere with LHC operations. We therefore assume the civil construction will be carried out mostly during LS3.

- The CERN accelerator safety group has concluded that the FPF can be accessed during LHC operations with appropriate controls for radiation safety. This will allow detector installation to proceed during Run 4.

- An important constraint is that detector construction, installation, and commissioning must happen before Run 4 concludes. This is quite important for the scientific productivity of the FPF and organization of the FPF community.

- We assume that the funding profile for the CERN infrastructure will follow the appropriate profile to allow start of detector installation in the 2029-2030 time frame.

- The funding profiles for other international contributions are not shown since they must follow the guidance of their respective funding agencies.

- We have included the costs for some of the additional infrastructure in the FPF cavern necessary for FLArE and FORMOSA into the US estimate in the US funding profile. Also no international cost sharing is assumed for items such as the cryostat and cryogenic systems.

- We assume that the US project will follow management and review schedules that are tailored for medium-scale projects according to the appropriate US national laboratory standard management system (for example, see Brookhaven National Laboratory SBMS [62]). In such management guidance, a CDR and a TDR review will be necessary before the full project funding can commence. Application of this standard will require discussion and agreement between the US collaborators, the national laboratories involved, and the US DOE. Therefore, full detector construction funding is assumed to start in FY2027. However, critical development, such as the FASER2 magnet systems, may require funding ahead of this date.

V. INTERNATIONAL PARTICIPATION

The FPF and the forward physics detector collaborations will follow the best governance practices established by other major collaborations such as ATLAS, CMS, DUNE, etc. An important difference between these major collaborations and the FPF community is the possibility of several

independent FPF scientific collaborations using the same facility and sharing resources. All of these collaborations will be international in nature.

Four of the proposed experiments, FASER2, FASERν2, Advanced SND, and FORMOSA, have pathfinder projects that are already installed and running at the LHC: FASER, FASERν, SND@LHC, and milliQan, respectively. MilliQan has already placed world-leading bounds on mCPs [61], and the first three experiments have taken data for the first time in 2022, leading to first results that have recently been presented at the 2023 winter conferences [1–4]. These results highlight the physics potential of the far-forward region, even with relatively modest luminosities and small experiments. The collaborations behind the existing experiments are creating a community for this science that will serve all experiments in the FPF.

Currently, the broader FPF experimental and theoretical community is approximately $\sim$400 strong (see the list of contributors to the recent white paper [14]). This community and additional scientists are expected to form the collaborations needed for the FPF experiments. The community is currently dominated by scientists from Europe, US, and Japan. Discussions to obtain R&D support from their respective agencies and institutions are in progress.

Along with the conceptual design report for the experiments and the facility, the community will propose a management structure under the guidance of CERN. This structure will need to have a strong technical coordination team to construct the facility according to the scientific requirements and also to install the detectors. Each of the scientific collaborations will have representation in the technical coordination team and will provide scientific resources as needed, and each collaboration will also seek coordination and resolution of overlapping requirements.

We expect the scientific collaborations to act independently to promote their respective science and detectors, and seek collaborators from CERN and the broader international particle physics communities. CERN has a longstanding procedure for accommodating such new collaborators, mainly from Europe and North America. For the FPF, we will attempt to broaden this to other parts of the world, especially in Asia, Africa, and the Americas. Such expansion will be welcome to inject new resources into this effort. Fortunately, the current program for forward physics has created a core community that is centered around the experiments FASER, FASERν, SND@LHC, and milliQan. This community is expected to lead the proposals for the FPF suite of experiments, but additional proposals that enhance the physics capabilities of the FPF are, of course, welcome.

Below we make some remarks about the status of the collaborations for each of the constituent experiments along with what is needed for further expansion:

- FASER2: The current FASER Collaboration has 87 members from 24 institutions in 10 countries [63]. FASER is a magnetized spectrometer (using permanent dipole magnets) that is housed in a service tunnel far-forward of ATLAS. It started taking data in Run 3. The FASER Collaboration is expected to form the core of the FASER2 effort. FASER2 will require a much larger effort towards an appropriate spectrometer magnet and a larger tracking system that can handle the trigger rates from HL-LHC. It also needs careful integration into the FPF hall and with the other experiments. The Collaboration will need to expand to bring in the appropriate technical expertise and resources for the larger effort.

- FASERν2: The FASERν2 collaboration will largely be made up from the existing FASERν experts who are part of the 87-person FASER Collaboration. The expertise on emulsion is mostly concentrated in Japan, where there is deep expertise and a strong tradition in using emulsion-based detectors for neutrino physics. Japan has the leading facilities for emulsion gel production and for the scanning of the emulsion films after exposure, and these will both be used in the FASERν2 operations.

- Advanced SND: The Advanced SND team will grow from the current SND@LHC Collaboration, which has 160 members from 23 institutes in 13 countries [64]. SND@LHC is a neutrino detector consisting of three main regions: a neutrino target with an embedded vertex detector and an electromagnetic calorimeter, a hadronic calorimeter, and a muon identification system consisting of scintillating bars with enough granularity to trace the muon tracks. Advanced SND will require a larger effort to cope with the HL-LHC environment.

- FLArE: FLArE is based on the liquid argon technology developed for the FNAL short baseline program, as well as DUNE. The FLArE collaboration will be based on the current working groups, which have approximately ∼50 participants, equally divided between US and European collaborators. The collaboration has recently received support from a private foundation, and a US national laboratory- (BNL-) directed R&D program. Because of the recent investment in DUNE prototypes, only limited and well-targeted R&D is needed for FLArE. Specifically, the readout electronics and pixel readout will need optimization for spatial resolution and dynamic range. Furthermore, trigger strategies will need to be developed for the FLArE geometry. The US collaboration is likely to have significant participation from US National Science Foundation (NSF)-supported groups. Such US-NSF contributions are not accounted for in the US estimate in Table II. At the moment, the collaboration has enough resources and person power to provide a physics proposal and a well-considered conceptual design. A modest-sized international collaboration (∼100 collaborators) with appropriate experience will have to be developed by the time of the technical design report in 2026.

- FORMOSA: FORMOSA would be based on the existing milliQan Collaboration with 29 members from 10 institutions in 5 countries [65]. The FORMOSA concept is based on well-known technology that requires limited R&D and is focused on mCPs. The US-based estimate assumes all capital investment from the US. Alterations and improvements to the design to substantially improve the detector sensitivity, such as through the use of alternative scintillator material, are under study, and the collaboration is expected to grow accordingly.

ACKNOWLEDGEMENTS

[1] **FASER** Collaboration, Petersen, Brian, "First Physics Results from the FASER Experiment."

https://indico.in2p3.fr/event/29681/contributions/122474/attachments/76425/110931/05-BPetersen-v1.pdf, 19 March 2023.

[2] **SND@LHC** Collaboration, Zaffaroni, Ettore, "Results of SND@LHC." https://indico.in2p3.fr/event/29681/contributions/122476/attachments/76427/110933/07-EZaffaroni-v1-public.pdf, 19 March 2023.

[3] **FASER** Collaboration, H. Abreu *et al.*, "First Direct Observation of Collider Neutrinos with FASER at the LHC," arXiv:2303.14185 [hep-ex].

[4] **FASER** Collaboration, "First Results from the Search for Dark Photons with the FASER Detector at the LHC," tech. rep., CERN, Geneva, 2023. https://cds.cern.ch/record/2853210.

[5] M. Narain *et al.*, "The Future of US Particle Physics - The Snowmass 2021 Energy Frontier Report," arXiv:2211.11084 [hep-ex].

[6] **European Strategy Group** Collaboration, *2020 Update of the European Strategy for Particle Physics*. CERN Council, Geneva, 2020.

[7] "Forward Physics Facility Kickoff Meeting." https://indico.cern.ch/event/955956, 9-10 November 2020.

[8] "2nd Forward Physics Facility Meeting (FPF2)." https://indico.cern.ch/event/1022352, 27-28 May 2021.

[9] "3rd Forward Physics Facility Meeting (FPF3)." https://indico.cern.ch/event/1076733, 25-26 October 2021.

[10] "4th Forward Physics Facility Meeting (FPF4)." https://indico.cern.ch/event/1110746, 31 January-1 February 2022.

[11] "5th Forward Physics Facility Meeting (FPF5)." https://indico.cern.ch/event/1196506, 15-16 November 2022.

[12] "Snowmass 2021." https://snowmass21.org, 2020-22.

[13] L. A. Anchordoqui *et al.*, "The Forward Physics Facility: Sites, experiments, and physics potential," *Phys. Rept.* **968** (2022) 1–50, arXiv:2109.10905 [hep-ph].

[14] J. L. Feng *et al.*, "The Forward Physics Facility at the High-Luminosity LHC," *J. Phys. G* **50** (2023) no. 3, 030501, arXiv:2203.05090 [hep-ex].

[15] **FASER** Collaboration, A. Ariga *et al.*, "Letter of Intent for FASER: ForwArd Search ExpeRiment at the LHC," arXiv:1811.10243 [physics.ins-det].

[16] B. Batell, J. L. Feng, and S. Trojanowski, "Detecting Dark Matter with Far-Forward Emulsion and Liquid Argon Detectors at the LHC," *Phys. Rev. D* **103** (2021) no. 7, 075023, arXiv:2101.10338 [hep-ph].

[17] S. Foroughi-Abari, F. Kling, and Y.-D. Tsai, "Looking forward to millicharged dark sectors at the LHC," *Phys. Rev. D* **104** (2021) no. 3, 035014, arXiv:2010.07941 [hep-ph].

[18] A. Berlin and F. Kling, "Inelastic Dark Matter at the LHC Lifetime Frontier: ATLAS, CMS, LHCb, CODEX-b, FASER, and MATHUSLA," *Phys. Rev. D* **99** (2019) no. 1, 015021, arXiv:1810.01879 [hep-ph].

[19] F. Kling, J.-L. Kuo, S. Trojanowski, and Y.-D. Tsai, "FLArE up dark sectors with EM form factors at the LHC forward physics facility," *Nucl. Phys. B* **987** (2023) 116103, arXiv:2205.09137 [hep-ph].

[20] **Particle Data Group** Collaboration, P. A. Zyla *et al.*, "Review of Particle Physics," *PTEP* **2020** (2020) no. 8, 083C01.

[21] **IceCube** Collaboration, M. G. Aartsen *et al.*, "Measurement of the multi-TeV neutrino cross section with IceCube using Earth absorption," *Nature* **551** (2017) 596–600, arXiv:1711.08119 [hep-ex].

[22] A. De Rujula and R. Ruckl, "Neutrino and muon physics in the collider mode of future accelerators," in *SSC Workshop: Superconducting Super Collider Fixed Target Physics*, pp. 571–596. 5, 1984. http://inspirehep.net/record/204753/files/p571.pdf.

[23] **FASER** Collaboration, H. Abreu *et al.*, "Technical Proposal: FASERnu," arXiv:2001.03073 [physics.ins-det].

[24] **SND@LHC** Collaboration, G. Acampora *et al.*, "SND@LHC: The Scattering and Neutrino Detector at the LHC," arXiv:2210.02784 [hep-ex].

[25] **Pierre Auger** Collaboration, A. Aab *et al.*, "Muons in Air Showers at the Pierre Auger Observatory: Mean Number in Highly Inclined Events," *Phys. Rev. D* **91** (2015) no. 3, 032003, arXiv:1408.1421 [astro-ph.HE]. [Erratum: Phys.Rev.D 91, 059901 (2015)].

[26] **Pierre Auger** Collaboration, A. Aab *et al.*, "Testing Hadronic Interactions at Ultrahigh Energies with Air Showers Measured by the Pierre Auger Observatory," *Phys. Rev. Lett.* **117** (2016) no. 19, 192001, `arXiv:1610.08509 [hep-ex]`.

[27] **EAS-MSU, IceCube, KASCADE Grande, NEVOD-DECOR, Pierre Auger, SUGAR, Telescope Array, Yakutsk EAS Array** Collaboration, H. P. Dembinski *et al.*, "Report on Tests and Measurements of Hadronic Interaction Properties with Air Showers," *EPJ Web Conf.* **210** (2019) 02004, `arXiv:1902.08124 [astro-ph.HE]`.

[28] **EAS-MSU, IceCube, KASCADE-Grande, NEVOD-DECOR, Pierre Auger, SUGAR, Telescope Array, Yakutsk EAS Array** Collaboration, D. Soldin, "Update on the Combined Analysis of Muon Measurements from Nine Air Shower Experiments," *PoS* **ICRC2021** (2021) 349, `arXiv:2108.08341 [astro-ph.HE]`.

[29] J. Allen and G. Farrar, "Testing models of new physics with UHE air shower observations," in *33rd International Cosmic Ray Conference*, p. 1182. 7, 2013. `arXiv:1307.7131 [astro-ph.HE]`.

[30] L. A. Anchordoqui, H. Goldberg, and T. J. Weiler, "Strange fireball as an explanation of the muon excess in Auger data," *Phys. Rev. D* **95** (2017) no. 6, 063005, `arXiv:1612.07328 [hep-ph]`.

[31] J. Albrecht *et al.*, "The Muon Puzzle in cosmic-ray induced air showers and its connection to the Large Hadron Collider," *Astrophys. Space Sci.* **367** (2022) no. 3, 27, `arXiv:2105.06148 [astro-ph.HE]`.

[32] L. A. Anchordoqui, C. G. Canal, F. Kling, S. J. Sciutto, and J. F. Soriano, "An explanation of the muon puzzle of ultrahigh-energy cosmic rays and the role of the Forward Physics Facility for model improvement," *JHEAp* **34** (2022) 19–32, `arXiv:2202.03095 [hep-ph]`.

[33] **IceCube-Gen2** Collaboration, M. G. Aartsen *et al.*, "IceCube-Gen2: the window to the extreme Universe," *J. Phys. G* **48** (2021) no. 6, 060501, `arXiv:2008.04323 [astro-ph.HE]`.

[34] V. V. Barinov *et al.*, "Results from the Baksan Experiment on Sterile Transitions (BEST)," *Phys. Rev. Lett.* **128** (2022) no. 23, 232501, `arXiv:2109.11482 [nucl-ex]`.

[35] R. Abdul Khalek *et al.*, "Science Requirements and Detector Concepts for the Electron-Ion Collider: EIC Yellow Report," *Nucl. Phys. A* **1026** (2022) 122447, `arXiv:2103.05419 [physics.ins-det]`.

[36] R. A. Khalek, J. J. Ethier, E. R. Nocera, and J. Rojo, "Self-consistent determination of proton and nuclear PDFs at the Electron Ion Collider," *Phys. Rev. D* **103** (2021) no. 9, 096005, `arXiv:2102.00018 [hep-ph]`.

[37] R. Abdul Khalek, R. Gauld, T. Giani, E. R. Nocera, T. R. Rabemananjara, and J. Rojo, "nNNPDF3.0: evidence for a modified partonic structure in heavy nuclei," *Eur. Phys. J. C* **82** (2022) no. 6, 507, `arXiv:2201.12363 [hep-ph]`.

[38] K. J. Eskola, P. Paakkinen, H. Paukkunen, and C. A. Salgado, "EPPS21: a global QCD analysis of nuclear PDFs," *Eur. Phys. J. C* **82** (2022) no. 5, 413, `arXiv:2112.12462 [hep-ph]`.

[39] **PDF4LHC Working Group** Collaboration, R. D. Ball *et al.*, "The PDF4LHC21 combination of global PDF fits for the LHC Run III," *J. Phys. G* **49** (2022) no. 8, 080501, `arXiv:2203.05506 [hep-ph]`.

[40] R. D. Ball, A. Candido, S. Forte, F. Hekhorn, E. R. Nocera, J. Rojo, and C. Schwan, "Parton distributions and new physics searches: the Drell–Yan forward–backward asymmetry as a case study," *Eur. Phys. J. C* **82** (2022) no. 12, 1160, `arXiv:2209.08115 [hep-ph]`.

[41] **ATLAS** Collaboration, M. Aaboud *et al.*, "Measurement of the W-boson mass in pp collisions at $\sqrt{s} = 7$ TeV with the ATLAS detector," *Eur. Phys. J. C* **78** (2018) no. 2, 110, `arXiv:1701.07240 [hep-ex]`. [Erratum: Eur.Phys.J.C 78, 898 (2018)].

[42] R. Abdul Khalek, S. Bailey, J. Gao, L. Harland-Lang, and J. Rojo, "Towards Ultimate Parton Distributions at the High-Luminosity LHC," *Eur. Phys. J. C* **78** (2018) no. 11, 962, `arXiv:1810.03639 [hep-ph]`.

[43] J. Boyd, M. Andreini, G. Arduini, K. Balazs, R. A. Bozzi, F. Cerutti, F. Corsanego, J.-P. Corso, L. Elie, A. Infantino, A. Navascues Cornago, J. A. Osborne, G. Peon, and M. Sabate Gilarte, "Update on the FPF Facility technical studies," `https://cds.cern.ch/record/2851822`.

[44] P. Christensen, L. Dysert, J. Bates, D. Burton, R. Creese, and J. Hollmann, "18-R-97 Cost Estimate Classification System – as applied in engineering, procurement, and construction for the process industries,".

[45] "FLUKA." `https://fluka.cern`.

[46] C. Ahdida *et al.*, "New Capabilities of the FLUKA Multi-Purpose Code," *Front. in Phys.* **9** (2022) 788253.

[47] G. Battistoni *et al.*, "Overview of the FLUKA code," *Annals Nucl. Energy* **82** (2015) 10–18.

[48] **FASER** Collaboration, H. Abreu *et al.*, "The FASER Detector," `arXiv:2207.11427 [physics.ins-det]`.

[49] **FASER** Collaboration, A. Ariga *et al.*, "FASER's physics reach for long-lived particles," *Phys. Rev. D* **99** (2019) no. 9, 095011, `arXiv:1811.12522 [hep-ph]`.

[50] H. Sato *et al.*, "Superconducting dipole magnet for samurai spectrometer," *IEEE Transactions on Applied Superconductivity* **23** (2013) no. 3, 4500308–4500308.

[51] **LHCb SciFi Tracker** Collaboration, P. Hopchev, "SciFi: A large Scintillating Fibre Tracker for LHCb," in *5th Large Hadron Collider Physics Conference*. 10, 2017. `arXiv:1710.08325 [physics.ins-det]`.

[52] S. Lee, M. Livan, and R. Wigmans, "Dual-Readout Calorimetry," *Rev. Mod. Phys.* **90** (2018) no. 2, 025002, `arXiv:1712.05494 [physics.ins-det]`.

[53] M. Antonello *et al.*, "Tests of a dual-readout fiber calorimeter with SiPM light sensors," *Nucl. Instrum. Meth. A* **899** (2018) 52–64, `arXiv:1805.03251 [physics.ins-det]`.

[54] **FASER** Collaboration, H. Abreu *et al.*, "Detecting and Studying High-Energy Collider Neutrinos with FASER at the LHC," *Eur. Phys. J. C* **80** (2020) no. 1, 61, `arXiv:1908.02310 [hep-ex]`.

[55] **FASER** Collaboration, H. Abreu *et al.*, "First neutrino interaction candidates at the LHC," *Phys. Rev. D* **104** (2021) no. 9, L091101, `arXiv:2105.06197 [hep-ex]`.

[56] A. Haas, C. S. Hill, E. Izaguirre, and I. Yavin, "Looking for milli-charged particles with a new experiment at the LHC," *Phys. Lett. B* **746** (2015) 117–120, `arXiv:1410.6816 [hep-ph]`.

[57] A. Ball *et al.*, "A Letter of Intent to Install a milli-charged Particle Detector at LHC P5," `arXiv:1607.04669 [physics.ins-det]`.

[58] **milliQan** Collaboration, A. Ball *et al.*, "Sensitivity to millicharged particles in future proton-proton collisions at the LHC with the milliQan detector," *Phys. Rev. D* **104** (2021) no. 3, 032002, `arXiv:2104.07151 [hep-ex]`.

[59] "Eljen Technology." `https://eljentechnology.com/products/plastic-scintillators/ej-200-ej-204-ej-208-ej-212`, Accessed: April 14, 2023.

[60] "Saint-Gobain." `https://www.crystals.saint-gobain.com/products/bc-408-bc-412-bc-416`, Accessed: April 14, 2023.

[61] **milliQan** Collaboration, A. Ball *et al.*, "Search for millicharged particles in proton-proton collisions at $\sqrt{s} = 13$ TeV," *Phys. Rev. D* **102** (2020) no. 3, 032002, `arXiv:2005.06518 [hep-ex]`.

[62] "BNL Standards Based Management Systems, Small and Medium sized project guidance." `https://intranet.bnl.gov`.

[63] "FASER." `https://faser.web.cern.ch`.

[64] "SND@LHC." `https://snd-lhc.web.cern.ch`.

[65] "milliQan." `https://u.osu.edu/milliqan`.